Available online at www.sciencedirect.com
ScienceDirect
Geochimica et Cosmochimica Acta 71 (2007) 3056–3069
Geochimica et Cosmochimica Acta
www.elsevier.com/locate/gca

An experimental study of the solubility and speciation of neodymium (III) fluoride in F-bearing aqueous solutions

Art A. Migdisov *, A.E. Williams-Jones

Department of Earth and Planetary Sciences, McGill University, 3450 University Street, Montréal, Que., Canada H3A 2A7

Received 4 December 2006; accepted in revised form 4 April 2007; available online 10 April 2007

Abstract

The solubility of neodymium (III) fluoride was investigated at temperatures of 150, 200 and 250 °C, saturated water vapor pressure, and a total fluoride concentration ($HF°_{aq} + F^-$) ranging from 2.0×10^{-3} to 0.23 mol/l. The results of the experiments show that Nd^{3+} and NdF^{2+} are the dominant species in solution at the temperatures investigated and were used to derive formation constants for NdF^{2+} and a solubility product for NdF_3. The solubility product of NdF_3 ($\log K_{sp} = \log a_{Nd^{3+}} + 3 \log a_{F^-}$) is -24.4 ± 0.2, -22.8 ± 0.1, and -21.5 ± 0.2 at 250, 200 and 150 °C, respectively, and the formation constant of NdF^{2+} ($\log \beta = \log a_{NdF^{2+}} - \log a_{Nd^{3+}} - \log a_{F^-}$) is 6.8 ± 0.1, 6.2 ± 0.1, and 5.5 ± 0.2 at 250, 200 and 150 °C, respectively. The results of this study show that published theoretical predictions significantly overestimate the stability of NdF^{2+} and the solubility of NdF_3.

The potential impact of the results on natural systems was evaluated for a hypothetical fluid with a composition similar to that responsible for REE mineralization in the Capitan pluton, New Mexico. In contrast to results obtained using the theoretical predictions of Haas [Haas J. R., Shock E. L., and Sassani D. C. (1995) Rare earth elements in hydrothermal systems: estimates of standard partial molal thermodynamic properties of aqueous complexes of the rare earth elements at high pressures and temperatures. *Geochim. Cosmochim. Acta* **59**, 4329–4350.], which indicate that NdF^{2+} is the dominant species in solution, calculations employing the data presented in this paper and previously published experimental data for chloride and sulfate species [Migdisov A. A., and Williams-Jones A. E. (2002) A spectrophotometric study of neodymium(III) complexation in chloride solutions. *Geochim. Cosmochim. Acta* **66**, 4311–4323; Migdisov A. A., Reukov V. V., and Williams-Jones A. E. (2006) A spectrophotometric study of neodymium(III) complexation in sulfate solutions at elevated temperatures. *Geochim. Cosmochim. Acta* **70**, 983–992.] show that neodymium chloride species predominate and that neodymium fluoride species are relatively unimportant. This suggests that accepted models for REE deposits that invoke fluoride complexation as the method of hydrothermal REE transport may need to be re-evaluated.

1. INTRODUCTION

Fluoride complexes are widely considered to control the hydrothermal mobilization of the Rare Earth Elements (e.g., Salvi and Williams-Jones, 1990; Williams-Jones et al., 2000; Wood and Ricketts, 2000), in large part because of theoretical predictions which suggest that at elevated temperatures these complexes are many orders of magnitude more stable than REE complexes with other ligands (Wood, 1990; Haas et al., 1995). However, these predictions were based on extrapolations from experimental data at ambient temperature, and have not been confirmed by high-temperature experiments. Indeed, only Bilal and Langer (1987, 1989) have published results of a high-temperature experimental study of the REE in fluoride-bearing solutions, and these authors did not report thermodynamic formation constants for REE fluoride complexes, although apparent formation constants can be interpreted from one of their graphs (Bilal and Langer, 1989). These values are over three orders of magnitude lower than predicted by

* Corresponding author. Fax: +1 514 398 4680.
E-mail address: artas@eps.mcgill.ca (A.A. Migdisov).

0016-7037/$ - see front matter © 2007 Elsevier Ltd. All rights reserved.
doi:10.1016/j.gca.2007.04.004

the data of Haas et al. (1995) and over four orders of magnitude lower than predicted by the data of Wood (1990). In view of this disagreement, the lack of other high-temperature experimental data on REE fluoride complexes and the assumed importance of fluoride complexation in the hydrothermal transport of REE, there is urgent need for reliable, experimentally determined values of the formation constants of REE fluoride complexes at elevated temperatures. This study builds on previous experimental studies by the authors of the complexation of REE with chloride and sulfate (Migdisov and Williams-Jones, 2002, 2006; Migdisov et al., 2006) and reports results of an experimental study of the speciation of Nd in fluoride-bearing solutions at temperatures of 150, 200 and 250 °C and the pressure of liquid-saturated water vapor.

2. METHODS

The experiments were performed in Teflon reactors (50 cm^3 test tubes supplied by Cole-Parmer), and involved measuring the solubility of synthetic crystalline NdF_3 (Alfa AEsar, 99.99%) in aqueous solutions containing variable concentrations of HF. Before each experiment, the autoclaves and Teflon reactors were purged of atmospheric air with a stream of nitrogen. Crystals of NdF_3 were suspended in the solutions using gold wire; the reactors were sealed with Teflon stoppers and heated to temperatures of 150, 200 and 250 °C in titanium autoclaves. In order to balance the pressure developed inside the reactors during the experiments with the pressure in the autoclaves, an aliquot of distilled water (sufficient to ensure the presence of liquid water under the conditions of the experiments) was placed in each autoclave (Fig. 1). Minor differences in pressure, occurring during heating and quenching of the autoclaves, were compensated by the flexibility of the reactor walls. Autoclave volumes were determined by filling with 25 °C distilled water from a flask, and weighing this flask before and after filling (±0.1 g). In a set of control experiments designed to test for leakage of the Teflon reactors, samples of the distilled water were collected after quenching, and analyzed for Nd and F by Inductively Coupled Plasma Mass Spectrometry (ICPMS) and Neutron Activation Analysis (NAA), respectively. These experiments yielded concentrations below the detection limit of the methods (0.05 ppb and 1 ppm, respectively), demonstrating that there was negligible exchange of Nd and F between the reactors and the autoclaves. Mass losses from the reactors (which never exceeded 5% and were generally <3%) were determined by weighing the latter before and after runs. We concluded that these losses were due to evaporation of water during quenching of the autoclaves and were not associated with any significant losses of Nd and F. Heating was performed in a Fisher Isotemp forced draft oven (model 838F), which was modified by adding an aluminum box with 1.5-cm-thick walls to reduce temperature gradients. Gradients were measured before each set of experiments using chromel–alumel thermocouples located at the top, bottom, and center of the oven, and were typically less than the accuracy of the thermocouples used in the measurements (<1 °C over the height of the oven; where the oven height is 45 cm).

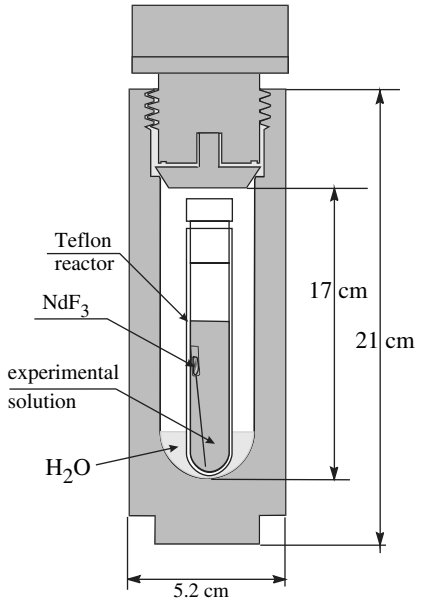

Fig. 1. A sketch of the experimental set-up used in this study. The autoclaves were constructed from titanium alloy (grade 2ASTM B348).

The solubility of neodymium (III) fluoride was investigated in acidic solutions ($pH_{25\,°C} = 1.2$–1.3 to avoid Nd hydrolysis, Wood et al., 2002) with a total fluoride concentration ($HF°_{aq} + F^-$) ranging from 2.0×10^{-3} (no fluoride added; concentrations developed due to NdF_3 dissolution) to 0.23 mol/l. Solutions were prepared using nano-pure de-ionized water (degassed in a nitrogen atmosphere) and HF, $HClO_4$ and $NaClO_4$ (Fisher Scientific, A.C.S.) in quantities appropriate to achieve the desired total fluoride concentration, acidity and ionic strength, respectively. Given the relatively small volume of gas (vapor) over the experimental solutions (~10 cm^3), as well as the low values of the Henry constants for HF^{gas} ($pK_H = 2.53$, 2.45, and 2.38 at 150, 200, and 250 °C, respectively; Reid et al., 1987) it can be concluded that 99.9% of the introduced HF remained in the aqueous liquid. In view of a study of Choppin et al. (1966), which demonstrated that the perchloric ion does not form detectable complexes with REE at concentrations below 6 mol/l, and given that concentrations of sodium perchlorate in the experimental solutions did not exceed 0.15 mol/l, it was assumed that any interaction of Nd with the perchloric ion was negligible at the conditions of the experiment. The experimental solutions were prepared in three sets so as to have concentrations of sodium perchlorate of 0.01, 0.05, and 0.15 mol/l, which, taking into account the concentrations of $HClO_4$, correspond to ionic strengths of 0.06, 0.1, and 0.2. In addition, in order to determine the time needed to reach equilibrium at each of the temperatures investigated, sets of experiments with durations varying from 1 to 5 days (kinetic runs) were performed under identical conditions (0.01 mol/l $NaClO_4$, no HF added) at 150, 200, and 250 °C (Fig. 2). It was found that detectable concentrations of Nd were present in the solutions after 12–20 h of heating. This, combined with

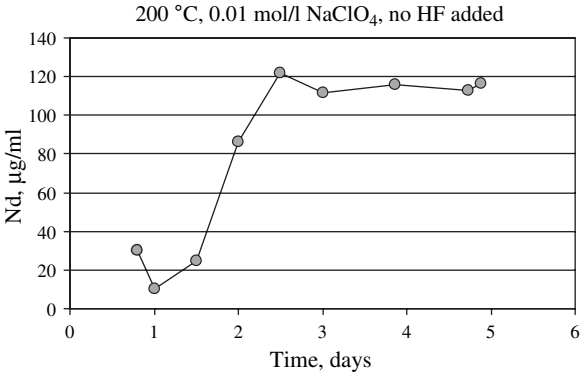

Fig. 2. An example of the solubility of NdF_3 as a function of time. The data suggest that equilibrium was attained after 2.5 days at 200 °C.

the fact that the thermal field of the oven stabilizes within ~1 h of the start of an experiment and that experiments are quenched to room temperature in <40 min, suggests that the concentrations measured correspond to those of isothermal solubility at the temperature of the experiment. The solubility of NdF_3 obtained in experiments conducted for durations exceeding 3 days was reproducible to approximately 7% at any temperature. After 4–5 days in the oven, the autoclaves were quenched in cold water, NdF_3 crystals were removed from the reactors, and the pH of the experimental solutions was determined potentiometrically. Determination of pH was performed using an AccuPH glass double junction electrode at 25 °C. The electrode was calibrated using a set of $NaClO_4/HClO_4$ solutions (pH = 1.0, 1.11, 1.17, 1.22, 1.31, 1.52 and 1.81) having a $NaClO_4$ concentration identical to that of the experimental solutions. Concentrations of $HClO_4$ in the solutions used for calibration were determined by titration with 0.01 M NaOH. Activity coefficients were calculated using the model developed by Hefter (1984) for acidic perchloric-based solutions. Given that HF is 99% associated at ambient temperature and at the conditions of the experiments, addition of HF to $HClO_4$ did not result in any detectable acidity changes. One to three milliliters of concentrated sulfuric acid was thereafter added to the solutions to dissolve any Nd precipitated on the inside walls of the Teflon reactors. The concentrations of Nd and F in the experimental solutions were determined using NAA (Ecole Politechnique, Montreal) and ICP-MS spectroscopy (Geochemical Labs, McGill; Activation Laboratories Ltd.). In order to ensure that Nd deposited on the walls of the reactor did not remain after sulfuric acid treatment, blank experiments (without NdF_3) were conducted after each series of runs. The blank experiments were treated in exactly the same manner as the rest of the experiments. Concentrations of Nd determined in blank runs (~0.03–0.05 ppb) were orders of magnitude lower than those determined in experimental solutions equilibrated with NdF_3 and were of the same level as the background concentrations of this element in sulfuric acid (~0.02 ppb) used to wash the reactors. In order to ensure that the measured solubility corresponded only to the dissolution of NdF_3, and was not affected by precipitation of another solid during the experiments, the crystals of neodymium fluoride were analyzed by X-ray diffraction; no other solid phases were detected.

3. RESULTS

The compositions of the experimental solutions after reaction with NdF_3 are listed in Table 1. At all temperatures investigated, the concentrations of Nd correlate negatively with fluoride concentrations. It was also found that the solubility of NdF_3 increases with temperature (for similar concentrations of HF).

The first step in our analysis of the data was to plot concentrations of Nd as a function of the activity of fluoride-ion (F^-). Fluoride-ion activity was calculated from the expression for the equilibrium constant for the dissociation of hydrofluoric acid

$$HF^\circ = H^+ + F^- \quad \log K_{HF} = \log a_{F^-} - pH - \log a_{HF}. \qquad (1)$$

The logarithm of the dissociation constant of HF ($\log K_{HF}$) was calculated for the saturated pressure of water vapor from the data of Johnson et al. (1992), which are based on dissociation constants for HF determined experimentally by Ryzhenko (1965) at 100, 156, and 218 °C. The values used in the calculations are −4.33, −4.86, and −5.44 at 150, 200 and 250 °C, respectively. Given that HF is a weak acid and under the experimental conditions is largely associated, calculations of fluoride activity require knowledge of the pH of the solutions at the temperature of the experiments. The latter was calculated assuming complete dissociation of $HClO_4$; the activity coefficient of the proton was calculated using the extended Debye–Hückel equation (Helgeson, 1969)

$$\log \gamma_n = \frac{A \cdot [z_n]^2 \cdot \sqrt{I}}{1 + B \cdot \dot{a} \cdot \sqrt{I}} + b \cdot I, \qquad (2)$$

where I is the ionic strength, z is the ion charge ($z_{H^+} = 1$), A and B are the Debye–Hückel coefficients (Helgeson, 1969; Helgeson et al., 1981), $\dot{a}$ is the distance of closest approach, which following Kielland (1937) was set at 9 Å. The value of b was set initially at the value of the extended parameter for a NaCl-based electrolyte (b_γ; Helgeson et al., 1981). However, this parameter was subsequently optimized for a $NaClO_4$-based electrolyte (see below). Activity coefficients for HF° were set at unity for each temperature investigated, and, given that under the experimental conditions concentrations of HF° are orders of magnitude greater than that of F^-, calculations of fluoride-ion activity were done assuming $\log a_{HF} = \log C_{HF}(\text{total})$.

The assumption that $HClO_4$ is completely dissociated was made due to the lack of any experimental data or theoretical predictions on ion pairing of this acid at elevated temperature. Potentially this can lead to some errors in the calculated pH, shifting it to more neutral values. However, if the ion pairing of $HClO_4$ is comparable to that of HCl, this shift should be insignificant compared to the other errors in the experiments (for error calculations see Section 4). For example, for a solution of HCl having $pH_{25\,^\circ C} = 1.3$ and ionic strength of 0.05 the effect of ion pairing on pH at 250 °C is only 0.02 U ($pH_{250\,^\circ C} = 1.42$ and 1.40 for models considering and not considering ion pairing, respectively).

Table 1
Compositions of the experimental solutions after equilibration with NdF_3

T °C	ClO_4^-	Na^+	$\sum$HF, 10^{-3}	$\sum$Nd, 10^{-7}	pH (25 °C)
	mol/l				
200	0.097	0.05	2.17	9513	1.32
200	0.097	0.05	2.83	5364	1.34
200	0.097	0.05	3.62	2000	1.34
200	0.097	0.05	4.57	1300	1.3
200	0.097	0.05	9.26	212	1.31
200	0.097	0.05	12.0	128	1.33
200	0.097	0.05	2.17	10,050	1.33
200	0.097	0.05	2.70	6650	1.33
200	0.097	0.05	2.63	4590	1.34
200	0.097	0.05	15.1	82.6	1.31
200	0.097	0.05	17.6	55.4	1.29
200	0.097	0.05	17.7	46.9	1.31
200	0.097	0.05	22.3	25.0	1.29
200	0.097	0.05	36.2	14.6	1.29
200	0.097	0.05	34.4	18.1	1.27
200	0.097	0.05	25.0	36.9	1.28
200	0.097	0.05	26.6	17.4	1.29
200	0.197	0.15	2.91	15,500	1.19
200	0.197	0.15	7.33	1330	1.13
200	0.197	0.15	12.1	583	1.05
200	0.197	0.15	7.71	1580	1.07
200	0.197	0.15	11.9	766	1.04
200	0.197	0.15	2.65	15,080	1.19
200	0.197	0.15	3.66	7250	1.17
200	0.197	0.15	8.25	666	1.17
200	0.197	0.15	8.83	833	1.17
200	0.197	0.15	16.7	141	1.17
200	0.197	0.15	35.4	33.2	1.15
200	0.057	0.01	2.97	3420	1.28
200	0.057	0.01	21.4	37.7	1.28
200	0.057	0.01	23.3	29.9	1.28
200	0.057	0.01	19.7	27.6	1.28
200	0.057	0.01	24.6	25.4	1.28
200	0.057	0.01	39.2	8.62	1.29
200	0.057	0.01	2.59	4670	1.29
200	0.057	0.01	27.1	20.0	1.28
200	0.057	0.01	30.5	14.2	1.28
200	0.057	0.01	32.1	13.5	1.26
200	0.057	0.01	39.4	9.43	1.29
200	0.057	0.01	35.7	9.89	1.28
200	0.057	0.01	1.96	11,370	1.29
200	0.057	0.01	32.4	16.3	1.28
200	0.057	0.01	59.4	3.60	1.28
200	0.057	0.01	63.8	3.40	1.29
200	0.057	0.01	75.4	2.46	1.29
200	0.057	0.01	74.8	2.09	1.29
200	0.057	0.01	2.02	9670	1.3
200	0.057	0.01	82.0	2.10	1.29
200	0.057	0.01	110.0	0.98	1.3
200	0.057	0.01	99.7	1.16	1.3
200	0.057	0.01	119.6	0.76	1.34
200	0.057	0.01	166.8	0.43	1.34
250	0.197	0.15	4.78	7050	1.21
250	0.197	0.15	25.0	117	1.21
250	0.197	0.15	37.1	41.1	1.19
250	0.197	0.15	43.7	39.7	1.2
250	0.197	0.15	39.9	39.9	1.2
250	0.197	0.15	52.2	27.5	1.21
250	0.197	0.15	6.41	3320	1.19
250	0.197	0.15	77.7	12.0	1.16

(*continued on next page*)

Table 1 (*continued*)

T °C	ClO_4^-	Na^+	$\sum$HF, 10^{-3}	$\sum$Nd, 10^{-7}	pH (25 °C)
	mol/l				
250	0.197	0.15	46.8	33.1	1.18
250	0.197	0.15	49.1	27.5	1.2
250	0.197	0.15	54.7	19.5	1.2
250	0.197	0.15	89.2	8.51	1.19
250	0.057	0.01	3.16	19,050	1.2
250	0.057	0.01	25.1	67.6	1.19
250	0.057	0.01	34.2	32.3	1.19
250	0.057	0.01	36.5	30.8	1.21
250	0.057	0.01	41.0	23.4	1.21
250	0.197	0.15	25.7	91.1	1.24
250	0.197	0.15	132.0	2.40	1.3
250	0.057	0.01	3.68	8440	1.23
250	0.057	0.01	5.07	2290	1.26
250	0.057	0.01	6.22	1410	1.25
250	0.057	0.01	8.99	796	1.21
250	0.057	0.01	9.14	478	1.24
250	0.057	0.01	71.6	7.39	1.23
250	0.057	0.01	65.5	6.91	1.23
250	0.057	0.01	140.6	1.62	1.28
250	0.057	0.01	204.9	0.56	1.32
250	0.097	0.05	3.22	11,980	1.27
250	0.097	0.05	3.39	11,430	1.26
250	0.097	0.05	14.7	166.67	1.23
250	0.097	0.05	10.7	583	1.18
250	0.097	0.05	19.5	95.6	1.23
250	0.097	0.05	68.6	10.4	1.23
250	0.097	0.05	69.7	7.76	1.28
250	0.097	0.05	132.1	1.12	1.39
250	0.097	0.05	136.3	1.00	1.46
250	0.097	0.05	230.4	0.12	1.65
150	0.057	0.01	1.90	6820	1.25
150	0.057	0.01	1.96	6010	1.26
150	0.057	0.01	1.64	7340	1.25
150	0.057	0.01	6.38	217	1.25
150	0.057	0.01	5.63	400	1.23
150	0.057	0.01	85.6	1.32	1.23
150	0.057	0.01	84.3	0.85	1.25
150	0.057	0.01	180.0	0.21	1.28
150	0.057	0.01	171.7	0.21	1.28
150	0.057	0.01	249.2	0.14	1.31
150	0.097	0.05	2.55	4550	1.21
150	0.097	0.05	2.41	6390	1.21
150	0.097	0.05	3.36	2020	1.21
150	0.097	0.05	3.78	1680	1.23
150	0.097	0.05	5.32	513	1.22
150	0.097	0.05	65.7	1.15	1.21
150	0.097	0.05	71.1	1.31	1.23
150	0.097	0.05	126.5	0.35	1.25
150	0.097	0.05	143.8	0.25	1.24
150	0.097	0.05	204.0	0.13	1.25

The values for ClO_4^- and Na^+ were calculated from the initial compositions of the solutions, $\sum$HF and $\sum$Nd are total concentrations of neodymium and fluorine determined after the runs.

Fig. 3a–c show logarithms of concentrations of Nd determined at 150, 200 and 250 °C, respectively, as a function of the logarithm of fluoride-ion activity. From these figures it can be seen that the solubility of NdF_3 increases slightly with increasing ionic strength. It is also evident that the concentration of Nd decreases linearly with increasing concentration of F and that the data can be subdivided into two distributions having slopes of approximately minus three and minus two at low and high fluoride concentration, respectively. This demonstrates that the solubility of NdF_3 is governed by two species, which are dominant over different intervals of fluoride concentration. The slope of −3 at low fluoride concentration corresponds to the simple dissociation reaction

$$NdF_3 = Nd^{3+} + 3F^- \quad \log K_{sp} = \log a_{Nd^{3+}} + 3\log a_{F^-}, \qquad (3)$$

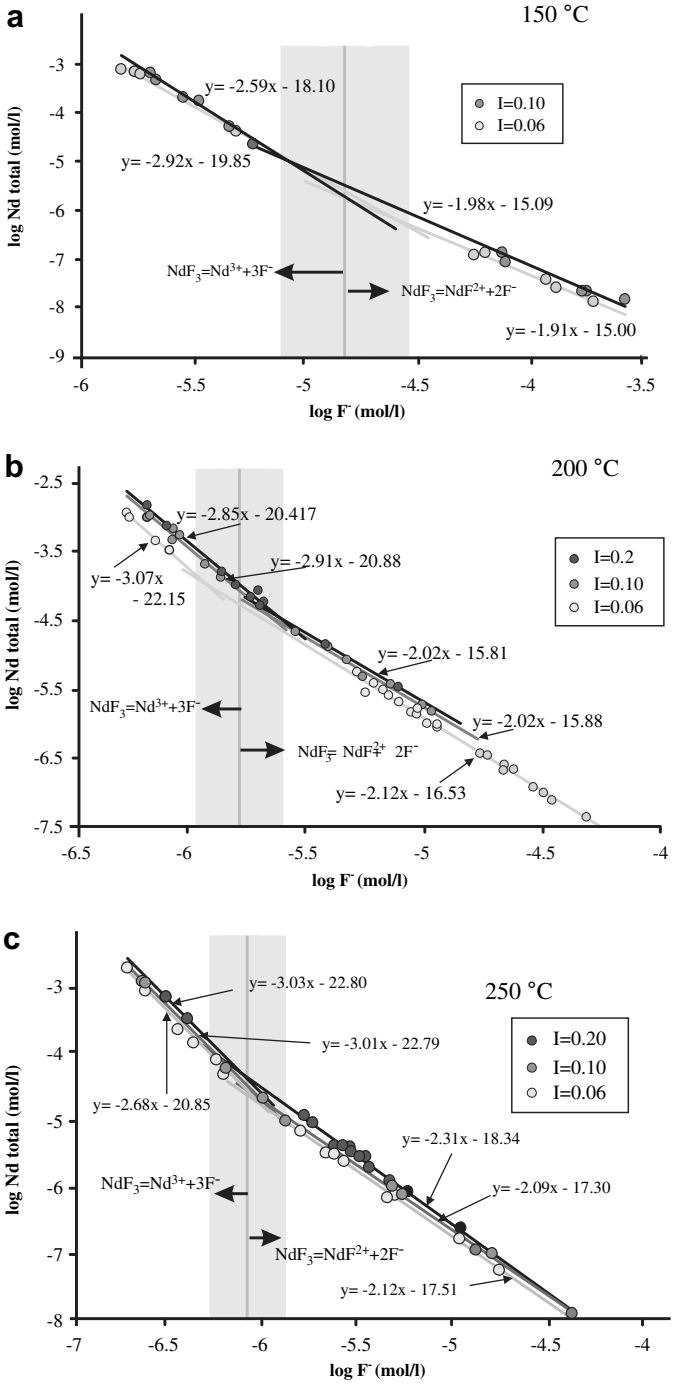

Fig. 3. Logarithms of Nd concentration determined at variable ionic strength (I) plotted as a function of the logarithm of the fluoride-ion activity at 150 (a), 200 (b) and 250 °C (c), respectively. The solid lines and corresponding equations represent linear regressions of the data. The vertical shaded area matches the locations of the predominance boundary between Nd^{3+} and NdF^{2+} at various ionic strengths.

whereas the slope of −2 reflects formation of the first fluoride complex of neodymium

$$NdF_3 = NdF^{2+} + 2F^- \quad \log K_{NdF^{2+}} = \log a_{NdF^{2+}} + 2\log a_{F^-}. \tag{4}$$

There is no evidence for the predominance of fluoride species with higher ligand numbers, like NdF_2^+ or $NdF_3°$, which would be reflected by data distributions with slopes of −1 and 0, respectively. It is possible that these species may predominate at fluoride concentrations higher than those in our experiments. However, it is unlikely that we would be able to detect these species if we were to extend our experiments to higher fluoride contents, as Nd concentrations would decrease to levels comparable to or below the detection limits of the analytical methods.

4. DATA TREATMENT

The dependencies illustrated in Fig. 3a–c can be used to determine equilibrium constants for reactions (3) and (4). However, the equations describing the dependencies shown in the figures (e.g., $\log C_{Nd^{3+}} = \log Q_{sp} - 3\log a_{F^-}$) represent expressions for apparent formation constants, derived for constant ionic strength and, as can be seen from the figures, change when the latter changes. In order to obtain thermodynamically valid formation and solubility constants, we employed an optimization procedure based on minimization of the overall error (U)

$$U = \sqrt{\sum_i \left(\frac{\log C_{Nd}^{Theo} - \log C_{Nd}^{exp}}{\log C_{Nd}^{exp}}\right)^2}, \quad (5)$$

where I is the number of experimental points in the dataset, C_{Nd}^{exp} is the concentration of Nd determined experimentally, and C_{Nd}^{Theo} is the concentration of Nd calculated theoretically using the values of the optimized constants, an optimized activity model and the total concentrations of fluoride and perchlorate.

Equilibrium constants were calculated for the reactions

$$NdF_3 = Nd^{3+} + 3F^-$$
$$\log K_{sp} = \log a_{Nd^{3+}} + 3\log a_{F^-}, \text{ (see Eq. (3))}$$

and

$$Nd^{3+} + F^- = NdF^{2+}$$
$$\log \beta = \log a_{NdF^{2+}} - \log a_{Nd^{3+}} - \log a_{F^-}. \quad (6)$$

The model also considered association Na–F due to ion pairing (which was insignificant). The activity of each species was calculated using the extended Debye–Hückel equation (Helgeson, 1969; Eq. (2)); the distances of closest approach for H^+, F^-, ClO_4^-, and Na^+, were set at 9, 3.5, 4.5 and 4 Å, respectively (Garrels and Christ, 1965; Langmuir, 1997). The equilibrium constants and b_{NaClO_4} were evaluated iteratively via successive minimization of the function U from initial guesses using MATLAB® software; the algorithm employed in the minimization was the Nelder–Mead simplex search described by Nelder and Mead (1965), and Dennis and Woods (1987).

The optimization was performed using two independent procedures. The first involved optimization of U with respect to K_{sp}, β, b_{NaClO_4} and distances of closest approach for Nd^{3+} and NdF^{2+} (Model A). In the second procedure, we optimized only K_{sp}, β, and b_{NaClO_4}, setting the distances of closest approach for Nd^{3+} and NdF^{2+} at 9 and 4.5 Å, respectively (Model B; Spedding et al., 1976; Gammons et al., 1996). Given that calculation of pH at the temperature of the experiments requires knowledge of H^+ activity at 25 °C, the parameter b for a $NaClO_4$-based electrolyte for 25 °C was also optimized (back-calculated) to provide the best fit to the experimental data. Uncertainties associated with the derivation of each of the values were calculated from the reproducibility of the results of kinetic experiments used to determine the time required to attain equilibrium. The distribution of the overall error for the treatment of the data was modeled as a function of the optimized parameter for each of the isotherms investigated, and was calculated using Eq. (5). Examples of these distributions are shown in Fig. 4a and b, respectively, as "profiles" of the overall error versus the values of the guessed formation constants. The optimized values of the formation constants correspond to the base of the depression in each profile. The figures also show the level representing the reproducibility of the results of the kinetic runs. Intersection of the profile with this level yields the uncertainty associated with the determination of each formation constant. The values obtained during the optimization are listed in Tables 2a and 2b.

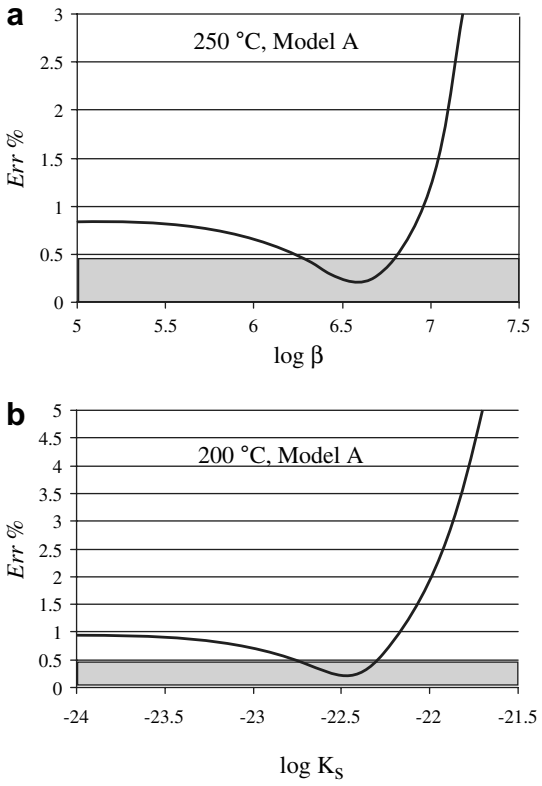

Fig. 4. Examples of the distribution of the overall error as a function of the optimized parameter. (a) Distribution of the overall error as a function of variations of the formation constant for NdF^{2+} at 250 °C (Model A); (b) distribution of the overall error as a function of variations of the solubility product of NdF_3 at 200 °C (Model A).

5. DISCUSSION

5.1. Model selection

As can be seen from Table 2, the values of the solubility product for NdF_3 (K_{sp}) obtained using Model A are indistinguishable from those using Model B at the level of uncertainty of the optimization. Similarly, variations of the distances of closest approach for Nd^{3+} and NdF^{2+} obtained in Model A are statistically insignificant (Fig. 5a), and can be assumed constant and equal to the values used in Model B; the values obtained in the two models for the

Table 2a
Values of the solubility product of NdF_3 ($\log K_{NdF_3}$; reaction 3) and the formation constant of NdF^{2+} ($\log\beta$; reaction 6) calculated using Model A and the data reported in Table 1

	250 °C	200 °C	150 °C
$\log K_{NdF_3}$	-24.26 ± 0.17	-22.76 ± 0.18	-21.60 ± 0.24
$\log\beta$	6.61 ± 0.17	6.17 ± 0.17	5.64 ± 0.22
b_{NaClO_4} (T)	0.13 ± 0.05	0.17 ± 0.05	0.19 ± 0.08
b_{NaClO_4} (25 °C)	0.19 ± 0.05	0.21 ± 0.06	0.21 ± 0.07
$\mathring{a}_{Nd^{3+}}$	9.5 ± 0.8	9.2 ± 0.8	9.1 ± 1.1
$\mathring{a}_{NdF^{2+}}$	4.0 ± 0.9	4.8 ± 0.8	5.0 ± 1.0

b_{NaClO_4} (T) and b_{NaClO_4} (25 °C) are the values of the extended parameter of the Debye–Hückel equation (Eq. (2)) optimized for $NaClO_4$ solutions at the temperatures of the experiments and 25 °C, respectively. $\mathring{a}_{Nd^{3+}}$ and $\mathring{a}_{NdF^{2+}}$ are distances of closest approach optimized for Nd^{3+} and NdF^{2+}, respectively (see the text for further explanations).

Table 2b
Values of the solubility product of NdF_3 ($\log K_{NdF_3}$; reaction 3) and the formation constant of NdF^{2+} ($\log\beta$; reaction 6) calculated using Model A and the data reported in Table 1

	250 °C	200 °C	150 °C
K_{NdF_3}	-24.40 ± 0.19	-22.83 ± 0.19	-21.47 ± 0.21
$\log\beta$	6.84 ± 0.18	6.24 ± 0.17	5.55 ± 0.20
b_{NaClO_4} (T)	0.16 ± 0.06	0.19 ± 0.06	0.21 ± 0.07
b_{NaClO_4} (25 °C)	0.24 ± 0.06	0.23 ± 0.07	0.24 ± 0.09
$\mathring{a}_{Nd^{3+}}$ (fixed)	9.0	9.0	9.0
$\mathring{a}_{NdF^{2+}}$ (fixed)	4.5	4.5	4.5

b_{NaClO_4} (T) and b_{NaClO_4}(25 °C) are the values of the extended parameter of the Debye–Hückel equation (Eq. (2)) optimized for $NaClO_4$ solutions at the temperatures of the experiments and 25 °C, respectively. $\mathring{a}_{Nd^{3+}}$ and $\mathring{a}_{NdF^{2+}}$ were not optimized and fixed at 9 and 4.5 Å, respectively (see the text for further explanations).

formation constants of NdF^{2+}(β) and b_{NaClO_4} are also indistinguishable within the estimated uncertainties (Fig. 5b and c). We therefore conclude that Model B, in which distances of closest approach for Nd^{3+} and NdF^{2+} were set at 9 and 4.5 Å, respectively, represents a best fit to the experimental data and increasing the complexity of the model does not improve the quality of the fit. Moreover, although the parameters of the activity model adopted in this study were evaluated for a relatively narrow range of ionic strengths (0.06–0.2), the values of b_{NaClO_4} (25 °C) obtained in the optimization agree reasonably well with those published previously in the literature. For example, Hefter (1984), who experimentally investigated the dissociation of HF in perchloric solutions at 25 °C and used the same approach as us to develop an activity model, reported values of b_{NaClO_4} (25 °C) as high as 0.29 for ionic strengths of up to 0.5, whereas our values derived for ambient temperature range between 0.19 and 0.21 (Table 2a and Fig. 5c). We do not exclude the possibility that the activity model developed in our study might not be applicable to higher ionic strengths (higher than 0.5). However, under the experimental conditions employed it provides a near perfect fit to the data (Fig. 6).

5.2. Activity model

In order to evaluate the significance of differences between the activity model derived in this study and models commonly employed for high-temperature solutions, we compared values of activity coefficients for Nd^{3+} (the species most sensitive to variation in ionic strength) obtained from our model with those calculated using the extended Debye–Hückel equation developed for NaCl-based solutions (b_{NaCl}; Oelkers and Helgeson, 1990) and the simplified Pitzer model (Pitzer and Kim, 1974; Harvie and Weare, 1980), which was developed by Millero (1992) for REE in ClO_4-based ambient temperature solutions. The latter model ignores ternary interactions and interactions of ions of the same charge (anion–anion, cation–cation), due largely to a lack of data for these parameters. Thus, in order to adopt this model to elevated temperatures, we used temperature derivatives for the ion interaction parameters from Silvester and Pitzer (1978) and Pitzer (1991); a more detailed description of the calculation is given in Migdisov and Williams-Jones (2006).

As can be seen from Fig. 7, the model derived in this study predicts activity coefficients for Nd^{3+} slightly lower than those obtained from the extended Debye–Hückel equation developed for NaCl-based solutions, but substantially higher than those calculated using the simplified Pitzer model. Moreover, whereas the NaCl-based Debye–Hückel equation shows relatively small and constant systematic deviations from the experimentally derived activity model, differences between the latter and the simplified Pitzer model increase sharply when temperature increases. Given the fact that the simplified Pitzer model has been shown to be suitable for ambient temperature (Millero, 1992), we speculate that the observed discrepancies are due either to poor extraction of the values of the ion interaction parameters at elevated temperatures or a more important role for

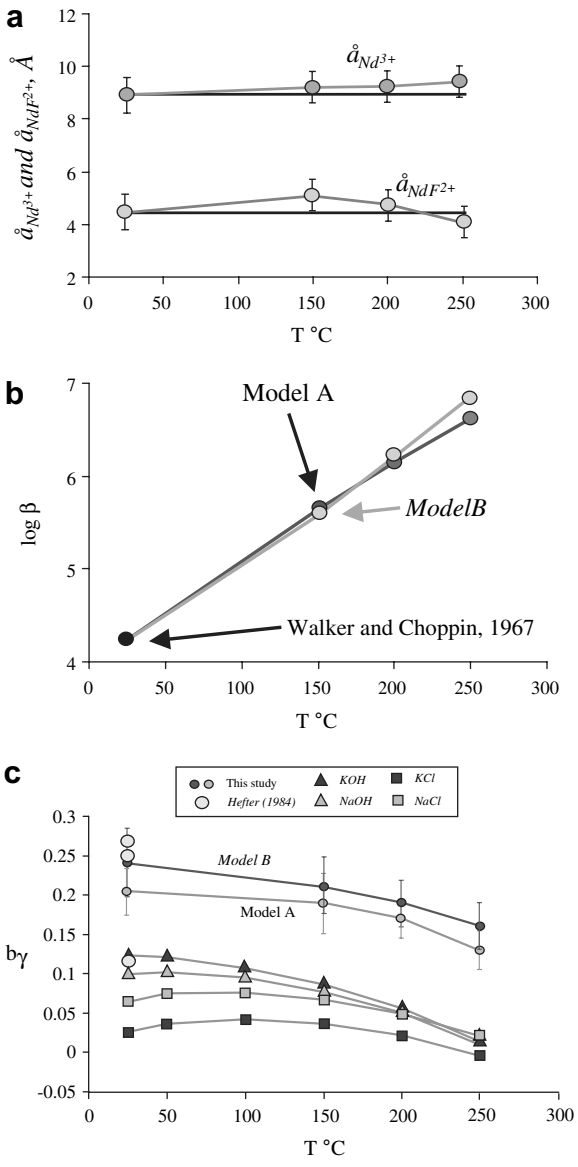

Fig. 5. (a) Variation with temperature of the optimized values for distances of closest approach for Nd^{3+} and NdF^{2+}. (b) Variation with temperature of the formation constant for NdF^{2+} calculated using Model A (black line) and Model B (grey line). (c) Values of the extended parameter of the Debye–Hückel equation (Eq. (2)) optimized for $NaClO_4$ solutions at the temperatures of the experiments and 25 °C, compared with the b_{NaClO_4} (25 °C) values from Hefter (1984), b_{NaCl} from Oelkers and Helgeson (1990), b_{KCl} from Pokrovskii and Helgeson (1997b), b_{NaOH} from Pokrovskii and Helgeson (1995), and b_{KOH} from Pokrovskii and Helgeson (1997a).

ternary interactions and interactions of ions of the same charge, which were ignored in the original model.

5.3. The solubility product of NdF_3

The only available study devoted to the thermochemical properties of NdF_3 at elevated temperatures is that of Lyon et al. (1979), which reported calorimetric measurements of the heat capacity of neodymium (III) fluoride at temperatures from 5 to 350 K. We fitted their data to the extended Mayer–Kelly equation

$$C_p\left(NdF_3, \mathrm{J\ mol^{-1}\ K^{-1}}\right) = 171.65 - 0.04851 \cdot TK - \frac{65660.37}{TK^2} - \frac{1148.39}{\sqrt{T}} + 3 \cdot 10^{-5} \cdot TK^2 \quad (7)$$

and calculated the solubility product of NdF_3 using the recommendations of the authors for $\Delta G°_f$ (298, NdF_3) = −1603.6 kJ mol^{-1}, $S°_f$ (298, NdF_3) = 120.79 J mol^{-1} K^{-1}, and data for Nd^{3+} and F^- recommended by Shock and Helgeson (1988) and Johnson et al. (1992), respectively. As is evident from Fig. 8, this calculated solubility product is about four orders of magnitude higher than the values derived in the present study and also compares poorly with 25 °C values published by Amano et al. (2004) and Baryshnikov and Gol'shtein (1972). In order to improve the agreement, we calculated a new value of the Gibbs free energy for NdF_3 from the data of Amano et al. (2004) based on the solubility of neodymium fluoride at 25 °C ($\Delta G°_f$ (298, NdF_3) = −1623.37 kJ mol^{-1}). This correction, however, yielded a calculated K_{sp} that was still over an order of magnitude higher than our experimentally determined value. In order to satisfactorily fit our data, it was therefore necessary to increase the entropy of neodymium fluoride from 120.79 to 179.3 J mol^{-1} K^{-1}.

It has to be mentioned that the possibility of formation of a monomolecular layer of a less soluble phase on the sur-

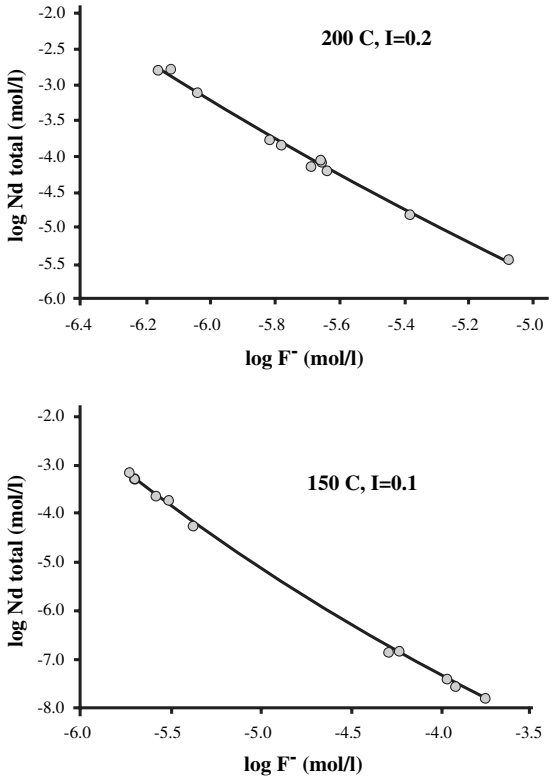

Fig. 6. Model B. Examples of fits to the experimental data using Model B at ionic strengths of 0.2 (a) and 0.1 (b).

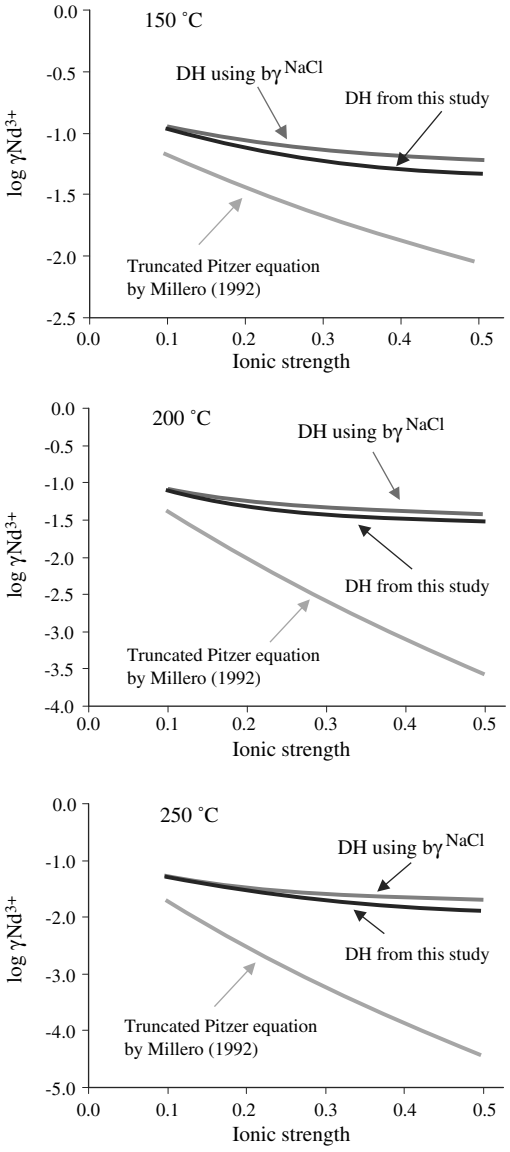

Fig. 7. Activity coefficients for Nd^{3+} calculated as a function of ionic strength using the model developed in this study, the extended Debye–Hückel equation developed for NaCl-based solutions, and the simplified Pitzer model developed by Millero (1992) for ambient-temperature solutions.

face of NdF_3 cannot be completely excluded for our runs. This layer would not be detected by XRD and, if CO_2 is not carefully purged from the system, could contain carbonates, hydrocarbonates, or hydroxybastnäsite-like substances. However, if any of these phases had formed during our runs, this would have led to non-stoichiometric slopes of dependencies in the co-ordinates log F/log Nd, which was not the case. We also consider it highly unlikely that hydroxyl or carbonate compounds formed under the extremely acidic conditions of our experiments.

5.4. The formation constant for NdF^{2+}

As was noted in the introduction to this paper, the only previous experimental study of neodymium fluoride com-

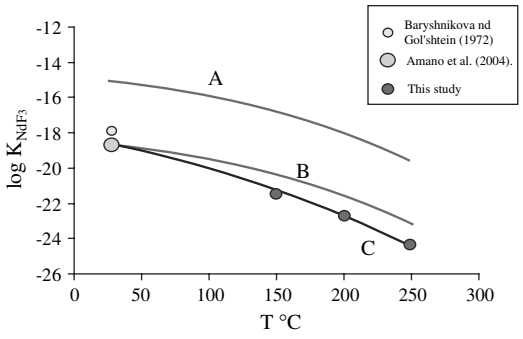

Fig. 8. Comparison of the values derived in this study for the solubility product of NdF_3 with those calculated based on published data in the literature. Line A was calculated using the Cp equation and entropy recommended by Lyon et al. (1979), and $\Delta G°_f(298)$ was also estimated by Lyon et al. (1979); Line B was calculated using the Cp equation and entropy recommended by Lyon et al. (1979), whereas $\Delta G°_f(298)$ was calculated from the solubility data of Amano et al. (2004). Line C represents calculations based on the Cp equation of Lyon et al. (1979), $\Delta G°_f(298)$ from Amano et al. (2004), and $S_{NdF_3}(298)$ from this study. The figure also shows experimentally determined values of the solubility product from this study and from ambient temperature studies of Amano et al. (2004) and Baryshnikov and Gol'shtein (1972). Error bars are smaller than the diameter of the dots on the figure.

plexation was that of Bilal and Langer (1987, 1989), who investigated the speciation of the REE over a range of F^- concentrations in a 1 M solution of NaCl at 1000 bars. Unfortunately, Bilal and Langer (1987, 1989) did not report any numerical data, but we were able to interpret an apparent formation constant for NdF^{2+} of 3.2 at 200 °C from one of their graphs (Bilal and Langer, 1989). In order to compare this value to the formation constant determined in our study for infinite dilution ($\log\beta = 6.2$) we used the latter to calculate an apparent formation constant for 200 °C and $I = 1$ based on the activity model described above. This calculation yielded a value of 5.5, which is more than two orders of magnitude larger than the value of Bilal and Langer (1987, 1989). Such a large disagreement cannot be attributed to a pressure dependency of the formation constant, nor to a potentially inaccurate (at high ionic strength) activity model. Unfortunately, as Bilal and Langer (1989) provided little information on their experimental method and only presented a graphical interpretation of their results, we were unable to determine the source of this disagreement.

Theoretical predictions of the values of the formation constant for NdF^{2+} were reported by Wood (1990) and Haas et al. (1995). In Fig. 9, we compare these predictions with the values obtained in our study. This figure shows that the theoretical predictions significantly overestimate the experimentally determined stability of NdF^{2+} at elevated temperature and that this disagreement increases with temperature. For example at 150 °C, the experimentally determined value of the formation constant is 0.4 orders of magnitude lower than that predicted by Haas et al. (1995), whereas at 250 °C, it is an order of magnitude lower. The disagreement with the predictions of Wood (1990) is even greater; his value at 250 °C is nearly three orders of

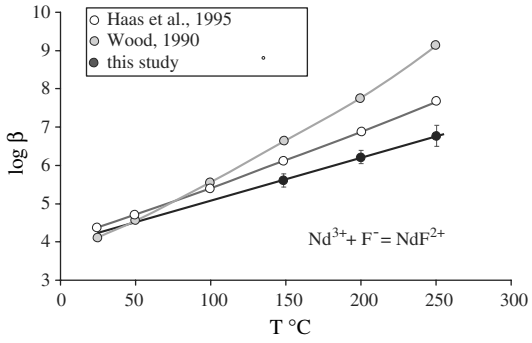

Fig. 9. Comparison of the values determined in this study for formation constant of NdF^{2+} with theoretical predictions of Wood (1990) and Haas et al. (1995).

Table 3
Parameters of the Ryzhenko–Bryzgalin model calculated for NdF^{2+}, $NdCl^{2+}$ and $NdCl_2^{+}$ based on the data presented in this study and Migdisov and Williams-Jones (2002)

Reaction	$pK^{298,1\ bar}$	A	B
$Nd^{3+} + F^- = NdF^{2+}$	4.344	0.257	543.9
$Nd^{3+} + Cl^- = NdCl^{2+}$	0.309	2.811	−938.5
$Nd^{3+} + 2Cl^- = NdCl_2^{+}$	0.031	2.783	−687.9

magnitude higher than our experimental value for the same temperature.

5.5. Application to natural systems

Hydrothermal transport of REE in natural systems is potentially controlled by several ligands, e.g., Cl^-, OH^-, F^- and SO_4^{2-}, and reliable evaluation of their relative importance depends on the availability of accurate estimates of formation constants for species involving these ligands. In order to illustrate how much the speciation changes depending on the choice of thermodynamic data, we modeled the speciation of Nd in a hypothetical fluid using the data presented here and in our previous experimental studies (Migdisov and Williams-Jones, 2002; Migdisov et al., 2006) and compared the results of this modeling with that based on thermodynamic properties of Nd species recommended by Haas et al. (1995). In order to approximate natural conditions, the fluid chosen for the modeling has a composition similar to that of fluid inclusions in REE-mineralized veins from the Capitan Pluton (New Mexico; Table 4), which were analyzed for their element content by Banks et al. (1994) and represent rare samples of a REE-saturated hydrothermal fluid for which the REE composition is now known. The U–Th-REE mineralization in this pluton occurs as thorite and allanite in quartz–barite–fluorite veins, containing minor amounts of feldspar and hematite and, based on fluid inclusion microthermometry, is interpreted to have deposited from high salinity magmatic brines at temperatures below 480 °C (the upper homogenization temperature limit of type 2 fluid inclusions; Banks et al., 1994).

Table 4
Composition of the fluid used to model the speciation of Nd in a hydrothermal fluid

Element	ppm
Na	192,438
K	61,409
Ca	30,723
F	1770
Cl	398,937
SO_4	24,210
Nd	190

The data were taken from the fluid inclusion study of the Capitan Pluton (New Mexico) of Banks et al. (1994).

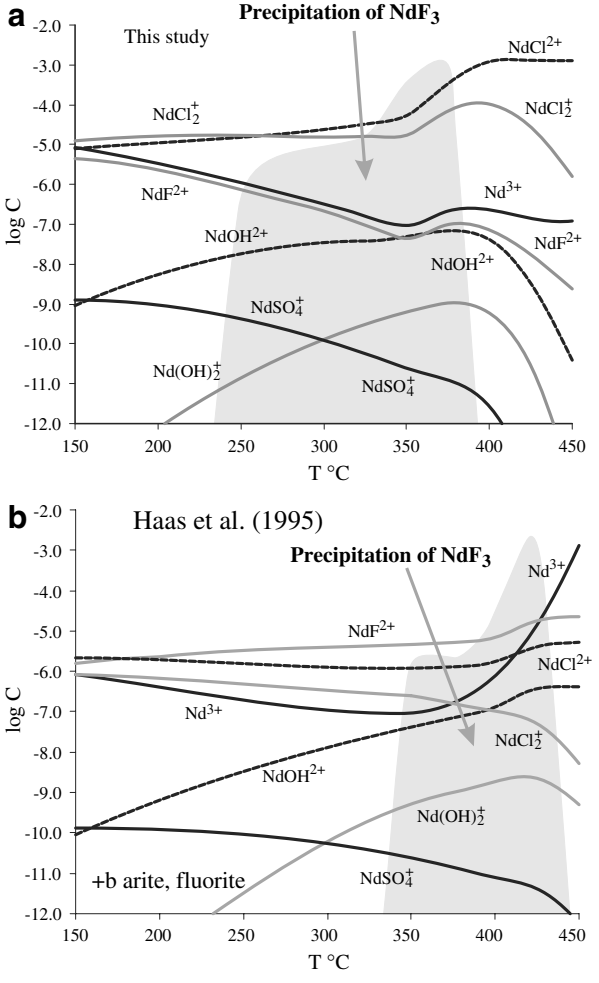

Fig. 10. Evolution of the aqueous speciation of Nd with temperature calculated using (a) the data obtained in this study and those of Migdisov and Williams-Jones (2002) and (b) the data recommended by Haas et al. (1995). The initial composition of the fluid was taken from the fluid inclusion study of the Capitan Pluton of Banks et al. (1994). The calculations assumed that the system was saturated with respect to barite and fluorite and that NdF_3 was the only neodymium-bearing solid to precipitate (see the text for an explanation).

We modeled the speciation of Nd for a solution flowing through a quartz–barite–fluorite vein (the fluid was therefore assumed to be saturated with respect to these minerals) as temperature decreased from 450 to 150 °C. The initial composition of the fluid is that given in Table 4 and the pressure was fixed at 500 bars. The solid phase hosting Nd was assumed to be NdF_3 and the initial pH of the solution was fixed at 4.0. A 1 l aliquot of the solution was equilibrated with 2 mol of the host minerals (quartz, barite and fluorite) at 450 °C and then, in a series of steps, was successively re-equilibrated with the fresh quartz–barite–fluorite assemblage as temperature decreased in 25 °C intervals. The solution composition was modeled using the following species: H^+, OH^-, $O_2°$, $H_2°$, Na^+, $NaOH°$, $NaHS°$, $NaSO_4^-$, $NaF°$, $NaCl°$, K^+, $KOH°$, KSO_4^-, $KHSO_4°$, $KCl°$, Ca^{2+}, $CaOH^+$, $CaSO_4°$, CaF^+, $CaCl^+$, $CaCl_2°$, Ba^{2+}, $BaOH^+$, BaF^+, $BaCl^+$, $H_2S°$, HS^-, $SO_2°$, SO_3^{2-}, HSO_3^-, SO_4^{2-}, HSO_4^-, $HS_2O_3^-$, $H_2S_2O_3°$, F^-, $HF°$, Cl^-, $HCl°$, Nd^{3+}, $NdOH^{2+}$, NdO^+, $NdSO_4^+$, NdF^{2+}, $NdCl^{2+}$, and $NdCl_2^+$. Thermodynamic properties for the species (except for Nd species other than Nd^{3+}, $NdOH^{2+}$ and NdO^+, which come from Haas et al., 1995) were taken from Johnson et al. (1992), Sverjensky et al. (1997), and Shock et al. (1989). The properties of water were determined using the Haar–Gallagher–Kell model (Kestin et al., 1984) and activity calculations were performed using the extended Debye–Hückel equation with the $b_{\gamma NaCl}$ extension parameter (Oelkers and Helgeson, 1990).

Experimentally determined formation constants for chloride and fluoride complexes of Nd (Migdisov and Williams-Jones, 2002; this study) were fitted to the modified Ryzhenko–Bryzgalin model (Ryzhenko, 1981; see Appendix A). In contrast to the multi-parametric HKF model, which cannot be applied to the data reported in the present study because of the small number of isotherms investigated, the modified Ryzhenko–Bryzgalin model requires only that the dissociation constant be known at 25 °C and one or two adjustable parameters employed to describe its temperature dependence. The parameters of the Ryzhenko–Bryzgalin model calculated for NdF^{2+}, $NdCl^{2+}$ and $NdCl_2^+$ are listed in Table 3. Formation constants for sulfate species of Nd were modeled using the data obtained by Migdisov et al. (2006), which were modified using the activity model derived in this study.

The distributions of Nd species calculated using the experimentally obtained data are shown in Fig. 10a and those calculated from the theoretical predictions of Haas et al. (1995) in Fig. 10b. Comparison of the diagrams shows that the two datasets predict very different distributions of Nd species. Whereas the model calculated from the data of Haas et al. (1995) predicts that Nd is transported primarily as a fluoride complex (NdF^{2+}) and that chloride complexation is minor, the model employing our experimental data predicts the predominance of Nd chloride species ($NdCl^{2+}$, $NdCl_2^+$) by orders of magnitude over any other Nd species. Moreover, given that fluoride is more susceptible to competition by complexation with other metals, such as Ca, Al, Fe, fluoride complexes may be even less important in real natural systems than a simple comparison of stability constants would suggest. It has to be noted, however, that the increased importance of chloride relative to fluoride in the calculations using our data is due not only to the stability of the fluoride complexes being substantially lower than predicted by Haas et al. (1995), but also due to the stability of the chloride complexes being higher (Migdisov and Williams-Jones, 2002) than theoretically predicted (Haas et al., 1995). As a result of the differences in speciation, the precipitation peak of neodymium fluoride occurs at between 450 and 325 °C in the model based on the data of Haas et al. (1995), whereas in the model using our experimental data it is between 375 and 225 °C.

It needs to be emphasized that the model discussed above is highly simplified and does not presume to establish the controls of REE mineralization in the Capitan Pluton. However it does demonstrate that the assumption of a dominant role for fluoride complexes, often made *a priori* by researchers interpreting the genesis of REE hydrothermal deposits, is not necessarily correct, and requires critical evaluation in light of the results of this study and that of Migdisov and Williams-Jones (2002).

6. CONCLUSIONS

The experimental data obtained in this study show that Nd^{3+} and NdF^{2+} are the dominant species in aqueous solutions at temperatures up to 250 °C and F^- concentrations higher than $10^{-4.5}$ mol/kg; NdF_2^+ was not detected. They also show that the theoretical predictions of Wood (1990) and Haas et al. (1995) significantly overestimate the stability of fluoride complexes of neodymium at elevated temperatures and that this overestimation increases with increasing temperature. Similarly, the solubility of neodymium (III) fluoride is lower than that predicted by thermodynamic data (Lyon et al., 1979). Using the data obtained in this study and previously published data for Nd–Cl species, it is now possible to evaluate the relative importance of fluoride and chloride complexation in natural systems and test earlier conclusions that fluoride species are the dominant agents of REE transport.

ACKNOWLEDGMENTS

This research was made possible through grants from NSERC and FQRNT to AEW-J. The manuscript benefited from thoughtful reviews by DC McPhail and two anonymous referees.

APPENDIX A

The modified Ryzhenko–Bryzgalin model, which was developed for extrapolation of dissociation constants, uses the same (or a similar) approach to the HKF model (Tanger and Helgeson, 1988), and expresses the free energy of any reaction as a sum of electrostatic and non-electrostatic terms. However, in contrast to the HKF model, for the case where electrostatic forces play a major role in interactions (ionic interaction of an anion *A* and a cation *B*), the model assumes the non-electrostatic term to be temperature- and pressure-independent. Employing the modified Born model, the modified Ryzhenko–Bryzgalin model expresses the free energy of dissociation and corresponding p*K* as follows:

$$\Delta_r G = \Delta_r G^{\text{non-electr.}} + \frac{|z^+ z^-| \cdot e^2 \cdot N}{(r_A + r_B) \cdot \varepsilon}, \quad (8)$$

$$\mathrm{p}K^{T,P} = \frac{298.15}{T}\mathrm{p}K^{298,1\text{ bar}} + \frac{e^2 \cdot N|z^+ z^-|}{\ln(10) \cdot R \cdot T \cdot a} \times \left(\frac{1}{\varepsilon_{T,P}} - \frac{1}{\varepsilon_{298,1\text{ bar}}}\right), \quad (9)$$

or

$$\mathrm{p}K^{T,P} = \frac{298.15}{T}\mathrm{p}K^{298,1\text{ bar}} + \Theta^{T,P}\left(\frac{|zz|}{a}\right)_{\text{eff}}. \quad (10)$$

Here, e stands for the electron charge, N is the Avogadro's number, ε is the dielectric constant of water at T and P and $a = r_A + r_B$ is the sum of the effective radii of the dissociation products, which is defined through the adjustable parameter

$$\left(\frac{|zz|}{a}\right)_{\text{eff}} = A + \frac{B}{T}. \quad (11)$$

The parameter $\Theta^{T,P}$ does not depend on the nature of the complex and is computed from the dissociation constant of water as described by Marshall and Franck (1981).

REFERENCES

Amano O., Sasahira A., Kani Y., Hoshino K., Aoi M., and Kawamura F. (2004) Solubility of lanthanide fluorides in nitric acid solution in the dissolution process of FLUOREX reprocessing system. *J. Nucl. Sci. Technol.* **41**, 55–60.

Banks D. A., Yardley B. W. D., Campbell A. R., and Jarvis K. E. (1994) REE composition of an aqueous magmatic fluid: a fluid inclusion study from the Capitan Pluton, New Mexico, USA. *Chem. Geol.* **113**, 259–272.

Baryshnikov N. V., and Gol'shtein T. V. (1972) Solubility of yttrium and neodymium fluorides in aqueous solutions of nitric and hydrochloric acids. *Nauch. Tr., Nauch.-Issled. Proekt. Inst. Redkometal. Prom.* **45**, 56–60.

Bilal B. A., and Langer P. (1987) Complex formation of trace elements in geochemical systems: stability constants of fluoro complexes of the lanthanides in a fluorite bearing model system up to 200 °C and 1000 bar. *Inorg. Chim. Acta* **140**, 297–298.

Bilal B. A., and Langer P. (1989) Complex formation of the lanthanides in fluorite-bearing hydrothermal solution. *Lanthanide Actinide Res.* **3**, 141–150.

Choppin G. R., Kelly D. A., and Ward E. E. (1966) Effect of changes in the ionic medium on the stability constant of $Eu(NO_3)^{2+}$. AEC Access. Nos., (ORO-1797-2), 21 pp.

Dennis J. E., Jr., and Woods D. J. (1987) In *New Computing Environments: Microcomputers in Large-Scale Computing* (ed. A. Wouk). SIAM, pp. 116–122.

Gammons C. H., Wood S. A., and Williams-Jones A. E. (1996) The aqueous geochemistry of the rare earth elements and yttrium: VI. Stability of neodymium chloride complexes from 25 to 300 °C. *Geochim. Cosmochim. Acta* **60**, 4615–4630.

Garrels R. M., and Christ C. L. (1965) *Solutions, Minerals, and Equilibria (Harper's Geoscience Series)*. Harper & Row, New York, 450 pp.

Haas J. R., Shock E. L., and Sassani D. C. (1995) Rare earth elements in hydrothermal systems: estimates of standard partial molal thermodynamic properties of aqueous complexes of the rare earth elements at high pressures and temperatures. *Geochim. Cosmochim. Acta* **59**, 4329–4350.

Harvie C. E., and Weare J. H. (1980) The prediction of mineral solubilities in natural waters: the Na–K–Mg–Ca–Sod–Cl–H_20 system from zero to high concentration at 25 °C. *Geochim. Cosmochim. Acta* **44**, 981–997.

Hefter G. T. (1984) Acidity constant of hydrofluoric acid. *J. Solut. Chem.* **13**, 457–470.

Helgeson H. C. (1969) Thermodynamics of hydrothermal systems at elevated temperatures and pressures. *Am. J. Sci.* **267**, 729–804.

Helgeson H. C., Kirkham D. H., and Flowers G. C. (1981) Theoretical prediction of the thermodynamic behavior of aqueous electrolytes at high pressures and temperatures: IV. Calculation of activity coefficients, osmotic coefficients, and apparent molal and standard and relative partial molal properties to 600 °C and 5 kb. *Am. J. Sci.* **281**, 1249–1516.

Johnson J. W., Oelkers E. H., and Helgeson H. C. (1992) SUPCRT 92: a software package for calculating the standard molal thermodynamic properties of minerals, gases, aqueous species, and reactions from 1 to 5000 bars and 0° to 1000 °C. *Comp. Geosci.* **18**, 899–947.

Kestin J., Sengers J. V., Kamgar-Parsi B., and Levelt-Sengers J. M. H. (1984) Thermophysical properties of fluid water. *J. Phys. Chem. Ref. Data* **13**, 175–183.

Kielland J. (1937) Individual activity coefficients of ions in aqueous solutions. *J. Am. Chem. Soc.* **59**, 1675–1678.

Langmuir J. (1997) *Aqueous Environmental Chemistry*. Prentice Hall, Inc., New Jersey.

Lyon W. G., Osborne D. W., and Flotow H. E. (1979) Thermodynamics of the lanthanide trifluorides. III. The heat capacity of neodymium trifluoride, NdF_3, from 5 to 350 K. *J. Chem. Phys.* **71**, 4123–4127.

Marshall W. L., and Franck E. U. (1981) Ion product of water substance, 0–1000 ° C, 1–10,000 bars, new international formulation and its background. *J. Phys. Chem. Ref. Data* **10**, 295–304.

Migdisov A. A., and Williams-Jones A. E. (2002) A spectrophotometric study of neodymium(III) complexation in chloride solutions. *Geochim. Cosmochim. Acta* **66**, 4311–4323.

Migdisov A. A., and Williams-Jones A. E. (2006) A spectrophotometric study of erbium (III) speciation in chloride solutions at elevated temperatures. *Chem. Geol.* **234**, 17–27.

Migdisov A. A., Reukov V. V., and Williams-Jones A. E. (2006) A spectrophotometric study of neodymium(III) complexation in sulfate solutions at elevated temperatures. *Geochim. Cosmochim. Acta* **70**, 983–992.

Millero F. J. (1992) Stability constants for the formation of rare earth inorganic complexes as a function of ionic strength. *Geochim. Cosmochim. Acta* **56**, 3123–3132.

Nelder J. A., and Mead R. (1965) A simplex method for function minimization. *Comput. J.* **7**, 308–313.

Oelkers E. H., and Helgeson H. C. (1990) Triple-ion anions and polynuclear complexing in supercritical electrolyte solutions. *Geochim. Cosmochim. Acta* **54**, 727–738.

Pitzer K. S. (1991) Ion interaction approach: theory and data correlation. In *Activity Coefficients in Electrolyte Solutions*, second ed. (ed. K. S. Pitzer). CRC Press, pp. 75–153.

Pitzer K. S., and Kim J. J. (1974) Thermodynamics of electrolytes. IV. Activity and osmotic coefficients for mixed electrolytes. *J. Am. Chem. Soc.* **96**, 5701–5707.

Pokrovskii V. A., and Helgeson H. C. (1995) Thermodynamic properties of aqueous species and the solubilities of minerals at high pressures and temperatures: the system Al_2O_3–H_2O–NaCl. *Am. J. Sci.* **295**, 1255–1342.

Pokrovskii V. A., and Helgeson H. C. (1997a) Thermodynamic properties of aq species and the solubilities of minerals at high

pressures and temperatures: the system Al_2O_3–H_2O–KOH. *Chem. Geol.* **137**, 221–242.

Pokrovskii V. A., and Helgeson H. C. (1997b) Calculation of the standard partial molal thermodynamic properties of KCl° and activity coefficients of aqueous KCl at temperatures and pressures to 1000 °C and 5 kbar. *Geochim. Cosmochim. Acta* **61**, 2175–2183.

Reid R. C., Prausnitz J. M., and Poling B. E. (1987) *The properties of gases and liquids*. McGraw-Hill, New York, 741 pp.

Ryzhenko B. N. (1981) *Thermodynamics of Equilibriums in Hydrothermal Solutions. (Termodinamika Ravnovesii v Gidrotermal'nykh Rastvorakh)*. Nauka, Moscow, USSR, 191 pp.

Ryzhenko B. N. (1965) Determination of dissociation constant of hydrofluoric acid and conditions of replacement of calcite by fluorite. *Geokhimiya* **3**, 273–276.

Salvi S., and Williams-Jones A. E. (1990) The role of hydrothermal processes in the granite-hosted zirconium, yttrium, REE deposit at Strange Lake, Quebec/Labrador: evidence from fluid inclusions. *Geochim. Cosmochim. Acta* **54**, 2403–2418.

Shock E. L., and Helgeson H. C. (1988) Calculation of the thermodynamic and transport properties of aqueous species at high pressures and temperatures: correlation algorithms for ionic species and equation of state predictions to 5 kb and 1000 °C. *Geochim. Cosmochim. Acta* **52**, 2009–2036.

Shock E. L., Helgeson H. C., and Sverjensky D. A. (1989) Calculation of the thermodynamic and transport properties of aqueous species at high pressures and temperatures: standard partial molal properties of inorganic neutral species. *Geochim. Cosmochim. Acta* **53**, 2157–2183.

Silvester L. F., and Pitzer K. S. (1978) Thermodynamics of electrolytes. X. Enthalpy and the effect of temperature on the activity coefficients. *J. Solut. Chem.* **7**, 327–337.

Spedding F. H., Weber H. O., Saeger V. W., Petheram H. H., Rard J. A., and Habenschuss A. (1976) Isopiestic determination of the activity coefficients of some aqueous rare earth electrolyte solutions at 25 °C. 1. The rare earth chlorides. *J. Chem. Eng. Data* **2**(1), 341–360.

Sverjensky D. A., Shock E. L., and Helgeson H. C. (1997) Prediction of the thermodynamic properties of aqueous metal complexes to 1000 °C and 5 kb. *Geochim. Cosmochim. Acta* **61**, 1359–1412.

Tanger, IV, J. C., and Helgeson H. C. (1988) Calculation of the thermodynamic and transport properties of aqueous species at high pressures and temperatures: revised equations of state for the standard partial molal properties of ions and electrolytes. *Am. J. Sci.* **288**, 19–98.

Williams-Jones A. E., Samson I. M., and Olivo G. R. (2000) The genesis of hydrothermal fluorite-REE deposits in the Gallinas Mountains, New Mexico. *Econ. Geol.* **95**, 327–341.

Wood S. A. (1990) The aqueous geochemistry of the rare-earth elements and yttrium. 2. Theoretical predictions of speciation in hydrothermal solutions to 350 °C at saturation water vapor pressure. *Chem. Geol.* **88**, 99–125.

Wood S. A., and Ricketts A. (2000) Allanite-(Ce) from The Eocene Casto Granite, Idaho: response to hydrothermal alteration. *Can. Mineral.* **38**(1), 81–100.

Wood S. A., Palmer D. A., Wesolowski D. J., and Benezeth, P. (2002) The aqueous geochemistry of the rare earth elements and yttrium. Part XI. The solubility of $Nd(OH)_3$ and hydrolysis of Nd^{3+} from 30 to 290 °C at saturated water vapor pressure with in-situ pH measurement. Special Publication—The Geochemical Society, (Water-Rock Interactions, Ore Deposits, and Environmental Geochemistry), 229–256.

Associate editor: Zhenhao Duan